European Archives of Oto-Rhino-Laryngology (2019) 276:1933–1941
https://doi.org/10.1007/s00405-019-05419-3

OTOLOGY

Imaging re-evaluation of the tympanic segment of the facial nerve canal using cone-beam computed tomography compared with multi-slice computed tomography

Zhengyu Zhang[1] · Hongxia Yin[1] · Zheng Wang[1] · Jing Li[1] · Han Lv[1] · Pengfei Zhao[1] · Zhenghan Yang[1] · Zhenchang Wang[1]

Received: 8 March 2019 / Accepted: 7 April 2019 / Published online: 2 May 2019

Abstract

Purpose This study aims to evaluate the imaging findings of cone-beam computed tomography (CBCT) in displaying subtle structures of the tympanic segment of the facial nerve canal in human cadaver heads compared with multi-slice computed tomography (MSCT).

Methods Between January 2017 and July 2017, images of the tympanic segment of the facial nerve canal acquired from 73 human cadaver ears by both CBCT and MSCT were prospectively studied. Then, images of the lateral and inferior walls of the tympanic segment were scored using standard imaging slices through a four-point rating scale. Subsequently, the detailed findings of these two imaging modalities were recorded and compared, including interruptions of the bony walls, thread-like bony tubes connected with the walls, and separations in the cavity. The Wilcoxon signed-rank test was used to investigate the differences between scores derived by CBCT and MSCT.

Results The mean score in the inferior and lateral walls by CBCT were significantly higher than that by MSCT ($P = 0.000$–0.005), which ranged from 2.0 (1.5, 2.5) to 3.5 (3.0, 4.0), and from 1.5 (1.0, 2.0) to 3.5 (2.5, 4.0), respectively. The interruption of the walls was most common at the anterior part of the inferior wall (38/73 cases). Furthermore, thread-like bony tubes were evident in 18 ears, which connected with the anterior part of the inferior wall (18/73 cases). Moreover, separation was found in 22 ears in the posterior part (22/73 cases).

Conclusions CBCT can readily demonstrate subtle imaging findings of the tympanic segment of the facial nerve canal.

Keywords Facial nerve canal · Cone-beam CT · Multislice computed tomography · Middle ear

Introduction

The facial nerve canal is a tortuous bony channel in the temporal bone that carries the temporal parts of the facial nerve. The tympanic segment is the second part of the facial nerve canal, which lies between the labyrinth (medially) and tympanic cavity (laterally) [1]. During middle ear surgery, the tympanic segment is the most common site for facial nerve injury, thereby requiring careful attention. Furthermore, the tympanic segment can also be involved in a number of other conditions, such as middle ear cholesteatoma and skull trauma, and is thereby one of the primary targets when analyzing temporal images.

With the advances in the precision medicine of facial nerve-related lesions, it has become increasingly apparent that new, more refined methods need to be developed to acquire and analyze detailed information relating to the facial nerve canal [2, 3]. After over 40 years of development, and due to advances directed at faster image acquisition and better spatial and contrast resolution, multi-slice computed tomography (MSCT) has increasingly been considered as the best option for imaging the facial nerve canal [4, 5]. However, to the best of our knowledge, none of the existing reports provide detailed MSCT information relating specifically to the tympanic segment of the facial nerve canal. Cone-beam computed tomography (CBCT) is a relatively new radiographic technique. Over the last decade,

✉ Zhenchang Wang
cjr.wzhch@vip.163.com

[1] Department of Radiology, Beijing Friendship Hospital, Capital Medical University, 95 Yong An Road, Western District, Beijing, China

differences in image acquisition beam shape, X-ray generator and detection system have highlighted CBCT as a better option than MSCT for dentomaxillofacial imaging [6–8]. Since CBCT imaging systems have become more widely available, and are continuously being upgraded, these are increasingly being used to image other anatomical regions, particularly in medical fields related to the head and neck [9–11]. The high spatial resolution and relatively low dose requirements render CBCT particularly attractive as an alternative to conventional MSCT [6, 9, 12].

In the experience of the investigators, due to the thinness of the lateral and inferior wall of the tympanic segment, these two walls can barely be identified by MSCT in the majority of cases. However, it is important to evaluate them in some conditions. Therefore, the investigators determined whether CBCT has the capability to define these thin walls of the facial nerve canal. In the present study, by compared with the images of MSCT, CBCT images were analyzed to evaluate the image quality of CBCT in demonstrating the detailed structures of the tympanic segment of the facial nerve canal.

Materials and methods

Between January 2017 and July 2017, 38 formalin-fixed human cadaver heads were consecutively scanned by a CBCT scanner (HiRes3D, LargeV, Beijing, China) and a MSCT scanner (Brilliance iCT, Philips Healthcare, Best, Netherlands). The age and gender of all specimens were unknown, and none of the specimens had a deformed appearance. The study was approved by the Institutional Review Board of the hospital.

Imaging techniques

CBCT imaging

The following imaging parameters were selected: voltage, 100 kV; current, 6 mA; exposure time, 12 s; voxel size, 0.1 mm; field of view (FOV), 5 × 8 cm; reconstruction increment, 0.1 mm; number of frames, 800. Images of the unilateral temporal bone were acquired after each scan.

MSCT imaging

The following imaging parameters were selected: voltage, 140 kV; current, 131 mA; pitch, 0.246; rotation time, 0.75 s; section collimation, 0.625 mm; matrix, 1024 × 1024; FOV, 18 cm; reconstruction slice thickness, 0.67 mm, reconstruction slice increment, 0.3 mm; number of frames, 180–244. The images were reconstructed using a bone algorithm [4]. A window width of 4000 Hu and a window center of 700 Hu were used. Images of the bilateral temporal bones were acquired after each scan.

After acquisition, both CBCT and MSCT scans were exported into DICOM file format and transferred to a three-dimensional (3D) workstation using a special software (RadiAnt DICOM Viewer 4.0.3; RadiAnt, Poland).

Image evaluation

CBCT and MSCT images were acquired from a total of 76 ears (38 specimens). Existing lesions that affected the facial nerve canal were identified in three of these ears and were excluded. Thus, the final analysis featured 73 ears. For each ear, CBCT and MSCT images were used to investigate the lateral and inferior walls, and the detailed structure of the tympanic segment of the facial nerve canal. This procedure was carried out in three steps, as detailed below.

Displaying the facial nerve canal and setting standard observation sections (Fig. 1) The axial/coronal/sagittal reformatting of each temporal bone was performed using the '3D MPR' function in RadiAnt software, and the following four steps were carried out.

a. On the axial images, the position line was adjusted to a locus, which was parallel to the tympanic segment. Then, the oblique sagittal images were acquired to clearly demonstrate the tympanic segment (Fig. 1a).
b. On the oblique sagittal images obtained from step (a), the position line was adjusted to a locus parallel to the tympanic segment, to adjust the axial images to follow the entire course of the tympanic segment (Fig. 1b).
c. On the coronal images, the position line was adjusted to a position that was as parallel as possible to the mastoid segment to further reconstruct the oblique sagittal images, on which the tympanic and mastoid segment could be simultaneously viewed (Fig. 1c).
d. The axial, oblique sagittal, and coronal images acquired in the previous three steps were used to evaluate the tympanic segment. Using the coronal images, position lines were placed in the center of the tympanic segment at the level of the cochleariform process (Fig. 1d). Then, standard slices were obtained from the axial and oblique sagittal images, and were used to observe and score the tympanic segment wall.

Scoring of the inferior and lateral wall of the tympanic segment The inferior and lateral wall of the tympanic segment was assessed using standard slices obtained from the oblique sagittal and axial images, respectively. The evaluation range was defined as a distance that extended from the posterior edge of the geniculate ganglion to the anterior edge of the pyramidal eminence. These two walls were both divided into

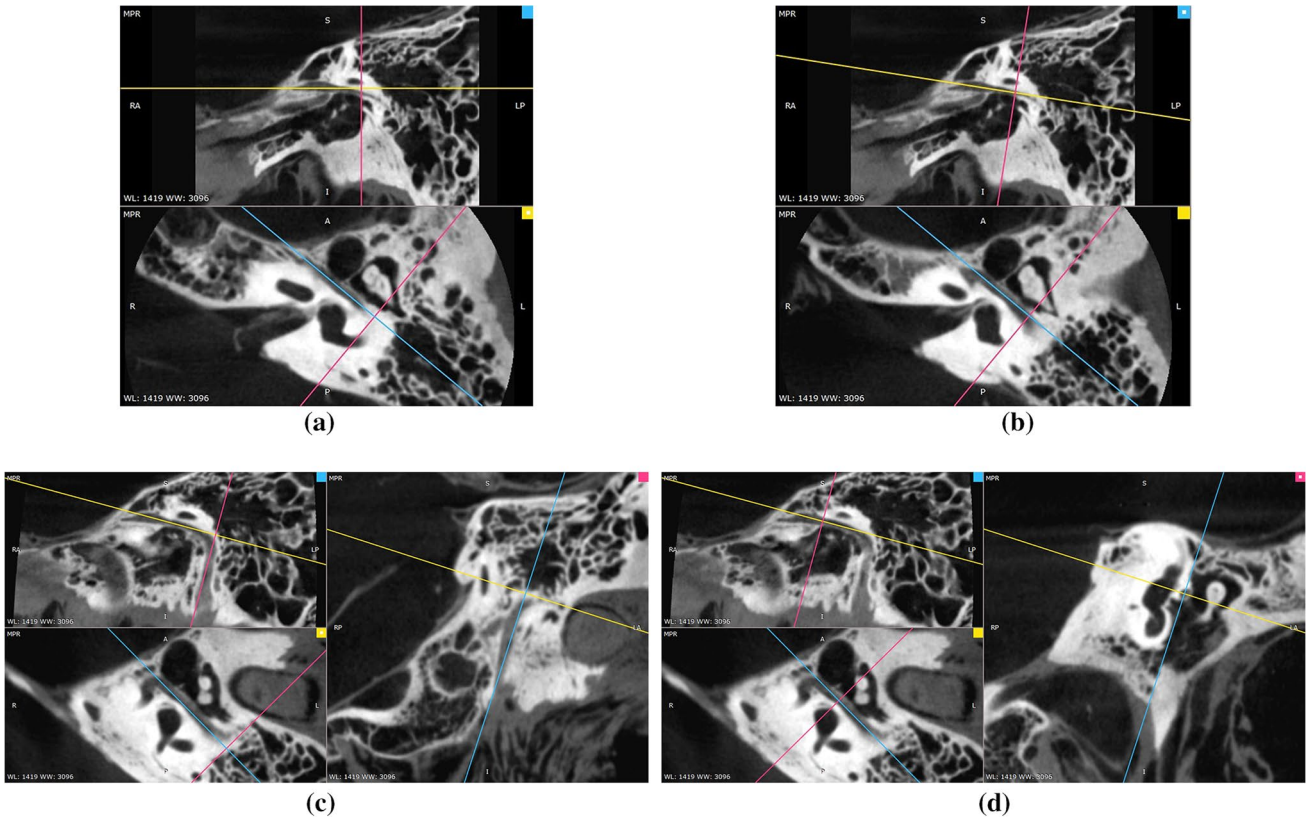

Fig. 1 CBCT of the facial nerve canal of left temporal bone. **a** Axial image (the lower image marked in yellow), the position line (blue) was parallel to the tympanic segment, and an oblique sagittal image was acquired (the upper image marked in blue). **b** Oblique sagittal image (the upper image marked in blue), the position line (yellow) was parallel to the tympanic segment, and an axial image was acquired (the lower image marked in yellow). **c** Coronal image (the right image marked in pink), the position line was as parallel as possible to the mastoid segment, and an oblique sagittal image (upper left image marked in blue) was finally acquired, on which the tympanic and mastoid segment are simultaneously shown. **d** Coronal image (the right image marked in pink), position lines were placed in the center of the tympanic segment at the level of the cochleariform process, and standard axial (lower left image marked in yellow) and oblique sagittal (upper left image marked in blue) images were obtained. *CBCT* cone-beam computed tomography

proximal and distal parts through the cochleariform process, and each part was separately evaluated (Fig. 1d). A four-point rating scale (Table 1) was used (Fig. 2).

One observer, who was a radiologist with 14 years of experience, assessed and scored all images twice with 1-week intervals between each evaluation to eliminate recall bias. The observer was blinded to all image acquisition details, and was allowed to adjust the brightness and contrast settings to obtain the best display.

Observing and recording the detailed findings obtained from the tympanic segment The four walls (inferior/lateral/superior/medial) of the tympanic segment were evaluated on both CBCT and MSCT images. Then, associated detailed presentations were recorded, including the interruption of walls, the thread-like bony tubes connected with the walls, and the separation within the canal. The same observer evaluated these images twice with a 1-week interval between each evaluation. Then, the CBCT and MSCT results were compared. If a difference was detected between these two imaging modalities, the images were evaluated again, and the four separate evaluations were combined to obtain a final result.

Table 1 Four-point rating scale used for the evaluation

Score	Evaluation	Imaging finding
1	Very poor	The wall could not be identified
2	Poor	The wall could be identified partly and incompletely
3	Acceptable	The wall could be identified completely with a blurred edge
4	Good	The wall could be identified completely with a relatively smooth edge

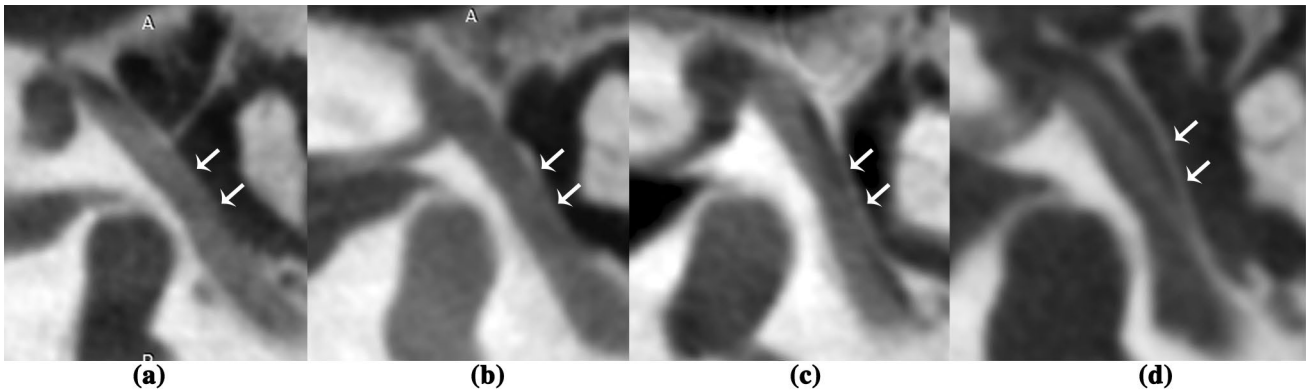

Fig. 2 Axial section acquired by CBCT of the tympanic segment of left temporal bone, and used to evaluate the lateral wall of the posterior part (arrows). **a** The wall could not be identified, and the image was very poor, scored 1. **b** The wall could be partly displayed, but the image was poor, scored 2. **c** The wall could be identified completely, and the edge was blurred, but the image was acceptable, scored 3. **d** The wall was displayed completely with a relatively smooth edge, and the image was good, scored 4. *CBCT* cone-beam computed tomography

Statistical analysis

All statistical analyses were carried out using the SPSS software (Version 17.0; SPSS, Inc, Chicago, IL, USA). Pearson correlation analysis was used to assess the inter-evaluation agreement of the scoring, and Wilcoxon signed-rank test was used to investigate differences between scores derived by CBCT and MSCT. The differences were considered significant when $P < 0.05$.

Results

Inter-evaluation agreement

Pearson correlation coefficient ranged from 0.687 to 0.759 for the first and second evaluation with $P = 0.000$, indicating that these two independent evaluations were identical and highly correlated.

Image quality

The medians and quartiles of the mean scores of the two measurements for the inferior and lateral walls of the tympanic segment in both CBCT and MSCT images are presented in Table 2. The scores were significantly higher by CBCT than by MSCT in all four parts of the walls ($P < 0.05$, Fig. 3). The medians and quartiles of the mean scores by CBCT and MSCT ranged from 2.0 (1.5, 2.5) to 3.5 (3.0, 4.0), and from 1.5 (1.0, 2.0) to 3.5 (2.5, 4.0), respectively. The box plots for the same data provided further confirmation of these findings (Fig. 4).

Detailed findings for the four walls of the tympanic segment

Bony interruption of the walls, thread-like bony tubes that connect with the walls and the separation within the cavity of the tympanic segment of the facial nerve canal were observed and recorded. The results are summarized in Table 3 and described below.

Table 2 Subjective image quality assessment of CBCT and MSCT images of the inferior and lateral walls of the tympanic segment ($n = 73$)

Walls of the tympanic segment	Median (quartiles)		Mean rank		*Z* value	*P* value
	CBCT	MSCT	Negative (MSCT < CBCT)	Positive (MSCT > CBCT)		
Anterior part of the inferior wall	3.5 (3.0, 4.0)	3.5 (2.5, 4.0)	24.57	17.50	− 3.978	0.000
Posterior part of the inferior wall	2.0 (1.5, 2.5)	1.5 (1.0, 2.0)	25.12	16.83	− 4.387	0.000
Anterior part of the lateral wall	3.0 (2.5, 3.5)	2.5 (2.0, 3.5)	29.17	19.06	− 3.471	0.001
Posterior part of the lateral wall	2.0 (1.5, 2.5)	2.0 (1.0,2.0)	25.42	19.53	− 2.795	0.005

CBCT cone-beam computed tomography, *MSCT* multi-slice computed tomography

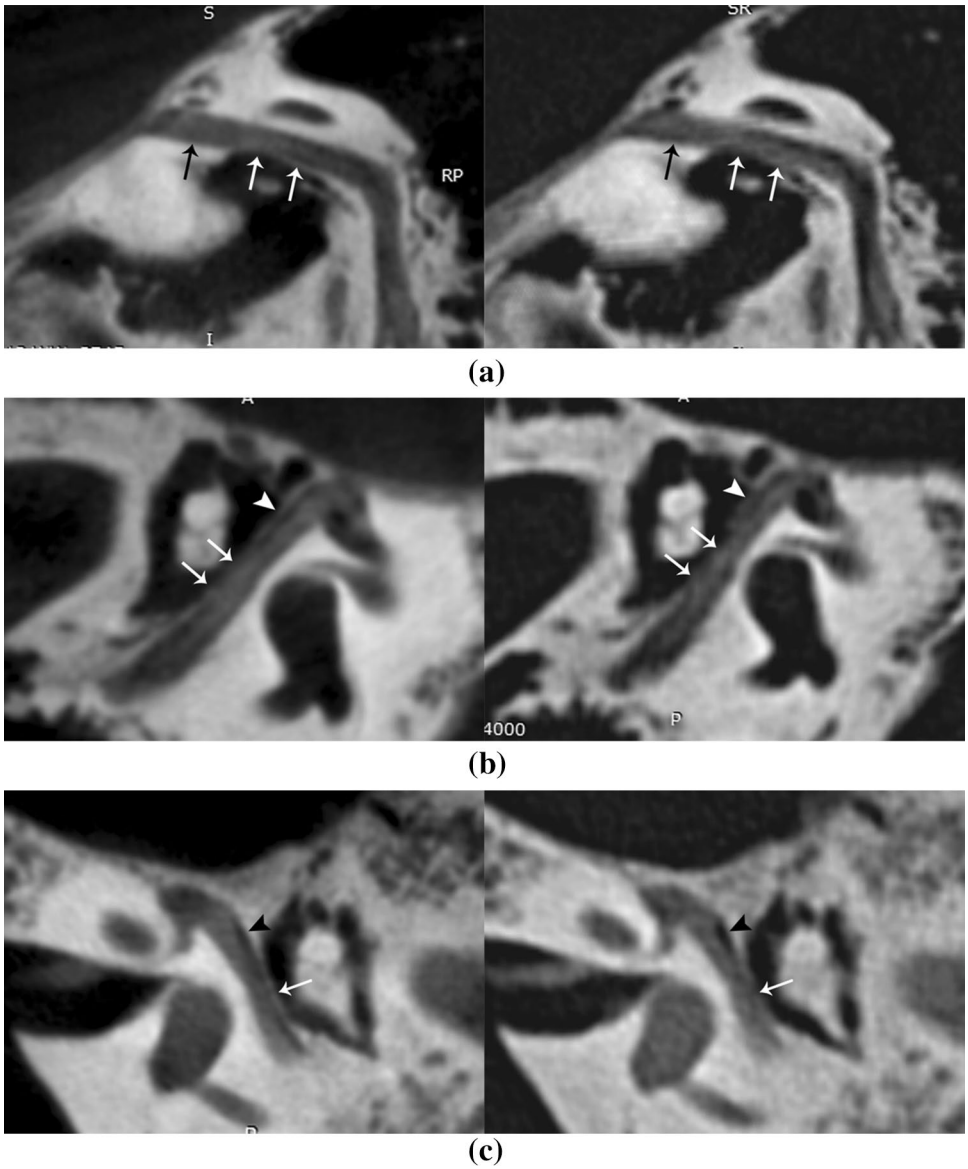

Fig. 3 The comparison of CBCT (left) and MSCT (right). **a** Oblique sagittal sections of the same case showed the anterior (black arrows) and posterior (white arrows) parts of the inferior wall. The image of the anterior part was good for both CBCT and MSCT (score: 4). The image of the posterior part was poor by CBCT (score: 2) and very poor by MSCT (score: 1). **b** Axial sections of the same case showed the anterior (arrowhead) and posterior (arrows) parts of the lateral wall. The image of the anterior part was acceptable by CBCT (score: 3), but was poor by MSCT (score: 2). The image of the posterior part was poor by CBCT (score: 2) and very poor by MSCT (score: 1). **c** Axial sections of the same case showed the anterior (arrowhead) and posterior (arrow) parts of the lateral wall. The image of the anterior part was good by both CBCT and MSCT (score: 4). The image of the posterior part was acceptable by CBCT (score: 3) and poor by MSCT (score: 2). *CBCT* cone-beam computed tomography, *MSCT* multi-slice computed tomography

Interruption of the walls was observed in many sites, which were most common (38 of 73 ears) in the anterior part of the inferior wall that connected with the tensor tympani canal (Fig. 5). The second most common site was in the superior wall between the facial nerve canal and lateral semicircular canal, and this was observed in 34 ears by CBCT and 38 ears (including the 34 ears observed by CBCT and the other four ears) by MSCT. This interruption was visualized as a tiny fissure that connects the facial nerve canal with the lateral semicircular canal, which could be observed on coronal and oblique sagittal sections. The third most common site was in the inferomedial wall adjacent to the oval window (detected in 31 ears by both CBCT and MSCT).

Thread-like bony tubes were identified in 18 ears by both imaging modalities. These tubes connected with the anterior part of the inferior wall of the facial nerve canal and ran close to the tensor tympani canal.

Separation was detected in 22 ears by both CBCT and MSCT in the posterior part of the tympanic segment of the facial nerve canal, which manifested as a high density blurry line. This structural feature was best observed in coronal sections.

Discussion

In the present study, the detailed image findings of the tympanic segment of the facial nerve canal were re-evaluated using both MSCT and CBCT. The present results demonstrate that the thin lateral and inferior walls of the tympanic segment could be displayed better by CBCT than by MSCT.

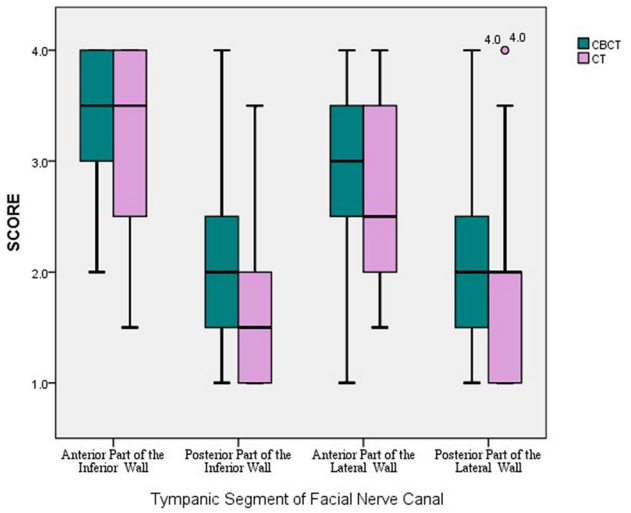

Fig. 4 Box plots of differences in scores between CBCT and MSCT in displaying the inferior and lateral walls of the tympanic segment of the facial nerve canal. The boxes represent the range of scores from the 25th to the 75th percentile. The horizontal bars indicate the medians, and the whiskers represent the 10th and 90th percentiles. The dots show the extremes. *CBCT* cone-beam computed tomography, *MSCT* multi-slice computed tomography

Some detailed findings were also observed in the tympanic segment by both CBCT and MSCT, including the interruption of walls, thread-like bony tubes that connected with the walls, and the separation within the canal.

Existing literature features several studies relating to the tympanic segment of the facial nerve canal. However, none of these studies described the bony walls of the tympanic segment in sufficient detail. For example, Tüccar et al. [13] described a bony lamella covering the tympanic segment in 14 (87.5%) specimens, but described this in a rather vague manner as either thick or very thin. In another study, Yu et al. [14] found that 33/67 (49.3%) of cases revealed an intact wall of the tympanic segment of the facial nerve canal on both CT images and by corresponding surgical findings, while the remaining 34 cases had dehiscence of the canal. Valavanis et al. [15] explored the facial nerve canal by high-resolution computed tomography (HRCT), and revealed that all segments of the facial nerve canal could be adequately demonstrated by this imaging modality when appropriate projections were used. However, the lower part of the bony wall of the tympanic segment was usually not visible.

For CBCT, relevant studies have been carried out. However, very few of these existing studies have focused upon the facial nerve canal [6–12, 16–22]. Komori et al. [22] used CBCT to measure the width of the normal facial canal, and found that CBCT measurements were similar to those obtained by cadaver dissection. This suggests that CBCT was a valuable tool for the measurement of narrow and minute bone structures.

In our study, two structures were observed to affect the walls of the anterior part of the tympanic segment. One was the tensor tympani canal, which is located under the tympanic segment, while the other is the supra-tubal recess [23], which is located lateral to the tympanic segment. Between the tensor tympani canal and tympanic segment is a dense bone with a certain thickness. The thickness of this bone is related to the location and course of the tensor tympani canal. If the tensor tympani canal is close and almost parallel to the tympanic segment of the facial nerve canal, the bony separation would be thin, and would likely to be difficult to image. The size of the supra-tubal recess was associated with the thickness of the lateral wall of the anterior part of the tympanic segment.

In the present study, the low scores derived from the walls of the posterior part of the tympanic segment, especially in the inferior wall, imply that most CBCT images of the posterior part of the inferior wall of the tympanic segment were poor, and that the wall could only be partially discernable, at best, although the scores by CBCT were higher than by MSCT. This has been considered to be related to low-energy

Table 3 Site and number of detailed imaging findings of the tympanic segment of the facial nerve canal ($n=73$)

Type	Site		Communication or location	*N* (CBCT/MSCT)	%
Interruption	Inferior wall	Anterior part	Tensor tympani canal	38/38	52.1
		Posterior part	Tympanic cavity	12/12	16.4
	Inferomedial wall		Near oval window	31/31	42.5
	Lateral and inferior wall		Same plane with oval window on coronal image	14/14	19.2
	Lateral wall	Posterior part	Tympanic cavity	4/4	5.5
	Superior wall	Posterior part	Lateral semicircular canal	34/38	46.6/52.1
Thread-like bony tube	Inferior wall	Anterior part	Near tensor tympani canal	18/18	24.7
	Superior wall	Anterior part		5/5	6.8
Separation		Posterior part		22/22	30.1

CBCT cone-beam computed tomography, *MSCT* multi-slice computed tomography

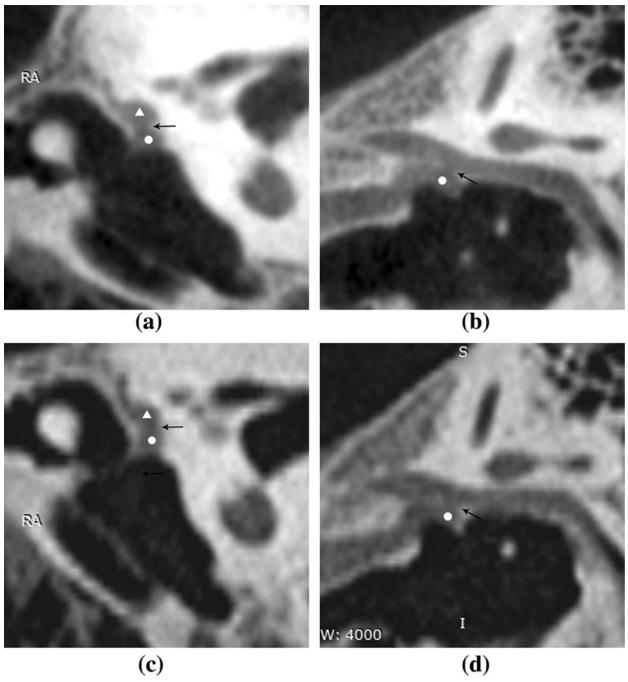

Fig. 5 Interruption (arrow) of the inferior wall of the tympanic segment (triangle) that connects with the tensor tympani canal (dot). The same case. **a**, **b** Coronal and oblique sagittal images acquired by CBCT. **c**, **d** Coronal and oblique sagittal images acquired by MSCT. The interruption was clearer by CBCT than by MSCT. *CBCT* cone-beam computed tomography, *MSCT* multi-slice computed tomography

photons and high noise signals associated with CBCT. Collectively, these features make it very difficult to image this extremely thin structure [10]. Consequently, a significant challenge for CBCT is to improve the signal-to-noise ratio, and increase the dose of radiation in a manner that would allow the demonstration of more subtle structures. Another reason for the poor imaging evident in the posterior part of the inferior wall is the dehiscence of the facial nerve canal at this region, which is a common occurrence, and may be mistakenly analyzed, thereby leading to low scores.

In the present study, the most common site of interruption observed was within the anterior part of the inferior wall, which separated the facial nerve canal from the tensor tympani canal, and most of the thread-like bony tubes were connected to the anterior part of the inferior wall. Such imaging findings have not been described in the literature. According to associated anatomical studies, the investigators considered that these findings may be related to the lesser petrosal nerve (LPN) and its communicating branches, and the courses of which significantly varies, making it very difficult to follow and study [24–28]. It is thereby evident that increased attention should be given to clinical imaging diagnosis when symptoms are suspected to be associated with LPN, or when surgery is planned in this particular region. Moreover, linear high density separations were identified in the posterior part of the cavity. This structure has not been previously mentioned in the literature. However, one study has reported a variation of the tympanic segment, that is, a bifid of the canal [29]. It is possible that these two independent findings depict the same change. According to the similar course of Arnold's nerve, which is one of the communicating branches of the LPN, one of the two separated parts in the facial nerve canal may represent Arnold's nerve. However, further investigations are now needed to clarify this [26].

The second most common site of interruption in the present study was within the superior wall between the facial nerve canal and lateral semicircular canal. Some of these interruptions were very obscure and could have been misdiagnosed. In four ears, MSCT provided positive detection, while CBCT did not. This may have been due to either the relatively low signal-to-noise ratio of the CBCT images, which masked this tiny change, or may have been due to MSCT overdiagnosis, as a result of artefacts. Furthermore, no previous reports have described this fissure between the facial nerve canal and lateral semicircular canal. At present, it remains unknown what the precise function of this fissure is, of if these fissures play a role in diseases and symptoms of the facial nerve and inner ear. Further research is required to address these shortfalls in our knowledge.

The presence of dehiscence in the facial nerve canal has been well-documented for many years [30–33]. According to literature, the tympanic segment, especially the area adjacent to the oval window, is the most common segment involved in dehiscence, and the present results were consistent with this. In addition to the dehiscence of the facial nerve canal, tiny orifices with vessels also emerged from the bony facial nerve canal [30, 33], which may be in accordance with the thread-like bony tubes observed in the present study.

The present study has some limitations that need to be considered when interpreting the results. First, the present analysis was based on images acquired from cadaver heads. Image quality can be affected by movement during clinical work, but was not a problem with the heads from cadavers. Second, the images were evaluated without comparison to anatomy. Future comparative studies with anatomy may confirm the detailed structures of the tympanic segment of the facial nerve canal, or merely lead to supposition.

In conclusion, the present study suggests that the imaging capability of CBCT is better than MSCT in terms of demonstrating the lateral and inferior walls of the tympanic segment of the facial nerve canal. Furthermore, both MSCT and CBCT can visualize the details of the tympanic segment of the facial nerve canal, including the interruptions of bony walls, thread-like bony tubes and separations in the cavity.

Funding This study was funded by National Natural Science Foundation of China (61527807 and 81371546); Natural Science Foundation of Beijing Municipality (7172064 and 7162048); Beijing Scholars Program [(2015)160]; Beijing Municipal Administration of Hospitals' Mission Plan (SML20150101); Beijing Municipal Science and Technology commission "Leading talent" Project (Z141107001514002).

Compliance with ethical standards

Conflict of interest The authors declare that they have no conflict of interest.

Ethical approval All procedures performed in studies involving human participants were in accordance with the ethical standards of the institutional research committee and with the 1964 Helsinki Declaration and its later amendments or comparable ethical standards.

Informed consent Not applicable.

References

1. Mortazavi MM, Latif B, Verma K, Adeeb N, Deep A, Griessenauer CJ, Tubbs RS, Fukushima T (2014) The fallopian canal: a comprehensive review and proposal of a new classification. Childs Nerv Syst 30:387–395. https://doi.org/10.1007/s00381-013-2332-0
2. Yadav SP, Ranga A, Sirohiwal BL, Chanda R (2006) Surgical anatomy of tympano-mastoid segment of facial nerve. Indian J Otolaryngol Head Neck Surg 58:27–30. https://doi.org/10.1007/BF02907734
3. Nikolaidis V, Nalbadian M, Psifidis A, Themelis C, Kouloulas A (2009) The tympanic segment of the facial nerve: anatomical study. Clin Anat 22:307–310. https://doi.org/10.1002/ca.20749
4. Chen JY, Mafee MF (2014) Computed tomography imaging technique and normal computed tomography anatomy of the temporal bone. Oper Tech Otolayngol Head Neck Surg 25:3–12. https://doi.org/10.1016/j.otot.2013.11.002
5. Ho ML, Juliano A, Eisenberg RL, Moonis G (2015) Anatomy and pathology of the facial nerve. AJR Am J Roentgenol 204:W612–W619. https://doi.org/10.2214/AJR.14.13444
6. Loubele M, Bogaerts R, Van Dijck E, Pauwels R, Vanheusden S, Suetens P, Marchal G, Sanderink G, Jacobs R (2009) Comparison between effective radiation dose of CBCT and MSCT scanners for dentomaxillofacial applications. Eur J Radiol 71:461–468. https://doi.org/10.1016/j.ejrad.2008.06.002
7. Nemtoi A, Czink C, Haba D, Gahleitner A (2013) Cone beam CT: a current overview of devices. Dentomaxillofacial Radiol 42:20120443. https://doi.org/10.1259/dmfr.20120443
8. Jain NV, Gharatkar AA, Parekh BA, Musani SI, Shah UD (2017) Three-dimensional analysis of the anatomical characteristics and dimensions of the nasopalatine canal using cone beam computed tomography. J Maxillofac Oral Surg 16:197–204. https://doi.org/10.1007/s12663-016-0879-5
9. De Cock J, Zanca F, Canning J, Pauwels R, Hermans R (2015) A comparative study for image quality and radiation dose of a cone beam computed tomography scanner and a multislice computed tomography scanner for paranasal sinus imaging. Eur Radiol 25:1891–1900. https://doi.org/10.1007/s00330-015-3593-7
10. Hodez C, Griffaton-Taillandier C, Bensimon I (2011) Cone-beam imaging: applications in ENT. Eur Ann Otorhinolaryngol Head Neck Dis 128:65–78. https://doi.org/10.1016/j.anorl.2010.10.008
11. Hatcher DC (2012) CT & CBCT imaging: assessment of the orbits. Oral Maxillofac Surg Clin N Am 24:537–543. https://doi.org/10.1016/j.coms.2012.07.003
12. Liang X, Jacobs R, Hassan B, Li L, Pauwels R, Corpas L, Souza PC, Martens W, Shahbazian M, Alonso A, Lambrichts I (2010) A comparative evaluation of cone beam computed tomography (CBCT) and multi-slice CT (MSCT) part I. On subjective image quality. Eur J Radiol 75:265–269. https://doi.org/10.1016/j.ejrad.2009.03.042
13. Tüccar E, Tekdemir I, Aslan A, Elhan A, Deda H (2000) Radiological anatomy of the intratemporal course of facial nerve. Clin Anat 13:83–87. https://doi.org/10.1002/(SICI)1098-2353(2000)13:2<3c83:AID-CA2>3e3.0.CO;2-Y
14. Yu Z, Wang Z, Yang B, Han D, Zhang L (2011) The value of preoperative CT scan of tympanic facial nerve canal in tympanomastoid surgery. Acta Otolaryngol 131:774–778. https://doi.org/10.3109/00016489.2011.554439
15. Valavanis A, Kubik S, Oguz M (1983) Exploration of the facial nerve canal by high-resolution computed tomography: anatomy and pathology. Neuroradiology 24:139–147
16. Casselman JW, Gieraerts K, Volders D, Delanote J, Mermuys K, De Foer B, Swennen G (2013) Cone beam CT: non-dental applications. JBR BTR 96:333–353
17. Güldner C, Diogo I, Bernd E, Dräger S, Mandapathil M, Teymoortash A, Negm H, Wilhelm T (2017) Visualization of anatomy in normal and pathologic middle ears by cone beam CT. Eur Arch Otorhinolaryngol 274:737–742. https://doi.org/10.1007/s00405-016-4345-2
18. Zou J, Lähelmä J, Arnisalo A, Pyykkö I (2017) Clinically relevant human temporal bone measurements using novel high-resolution cone-beam CT. J Otol 12:9–17
19. Penninger RT, Tavassolie TS, Carey JP (2011) Cone-beam volumetric tomography for applications in the temporal bone. Otol Neurotol 32:453–460. https://doi.org/10.1097/MAO.0b013e31820d962c
20. Peltonen LI, Aarnisalo AA, Käser Y, Kortesniemi MK, Robinson S, Suomalainen A, Jero J (2009) Cone-beam computed tomography: a new method for imaging of the temporal bone. Acta Radiol 50:543–548. https://doi.org/10.1080/02841850902839700
21. Akbulut N, Kursun S, Aksoy S, Kurt H, Orhan K (2014) Evaluation of foramen tympanicum using cone-beam computed tomography in orthodontic malocclusions. J Craniofac Surg 25:e105–e109. https://doi.org/10.1097/SCS.0000000000000440
22. Komori M, Yamada K, Hinohira Y, Aritomo H, Yanagihara N (2013) Width of the normal facial canal measured by high-resolution cone-beam computed tomography. Acta Otolaryngol 133:1227–1232. https://doi.org/10.3109/00016489.2013.816443
23. Yang B, Zhang F, Jiang X (2011) Imageology study of the relationship between supratubal recess and the course of cholesteatoma. Chin J Otol 9:136–138
24. Mavridis IN, Pyrgelis ES (2016) Clinical anatomy of the lesser petrosal nerve. Arch Neurosci 3:e34168. https://doi.org/10.5812/archneurosci.34168
25. Kakizawa Y, Abe H, Fukushima Y, Hongo K, El-Khouly H, Rhoton AL Jr (2007) The course of the lesser petrosal nerve on the middle cranial fossa. Neurosurgery 61:15–23. https://doi.org/10.1227/01.neu.0000289707.49684.a3
26. Vidić B (1968) The origin and the course of the communicating branch of the facial nerve to the lesser petrosal nerve in man. Anat Rec 162:511–516. https://doi.org/10.1002/ar.1091620413
27. Porto AF Jr, Whicker J, Proud GO (1978) An anatomic study of the hypotympanic branch of Jacobson's nerve. Laryngoscope 88:56–60
28. Kanzara T, Hall A, Virk JS, Leung B, Singh A (2014) Clinical anatomy of the tympanic nerve: a review. World J Otorhinolaryngol 4:17–22. https://doi.org/10.5319/wjo.v4.i4.17

29. Toulgoat F, Sarrazin JL, Benoudiba F, Pereon Y, Auffray-Calvier E, Daumas-Duport B, Lintia-Gaultier A, Desal HA (2013) Facial nerve: from anatomy to pathology. Diagn Interv Imaging 94:1033–1042. https://doi.org/10.1016/j.diii.2013.06.016
30. Baxter A (1971) Dehiscence of the fallopian canal. An anatomical study. J Laryngol Otol 85:587–594
31. Di Martino E, Sellhaus B, Haensel J, Schlegel JG, Westhofen M, Prescher A (2005) Fallopian canal dehiscences: a survey of clinical and anatomical findings. Eur Arch Otorhinolaryngol 262:120–126. https://doi.org/10.1007/s00405-004-0867-0
32. Faramarzi M, Roosta S (2017) Incidence of facial nerve canal dehiscence in primary and revision cholesteatoma surgery. Indian J Otolaryngol Head Neck Surg 69:300–306. https://doi.org/10.1007/s12070-017-1094-5
33. Perez B, Campos ME, Rivero J, Lopez Campos D, López-Aguado D (1997) Incidence of dehiscences in the fallopian canal. Int J Pediatr Otorhinolaryngol 40:51–60